

Cheating and imperfect vaccines as drivers of bacterial evolution

Florian Lecorvaisier^{1*}, Thomas L. P. Martin²

¹ Université Lyon 1, VetAgro Sup, CNRS, LBBE, UMR 5558, Villeurbanne, France

² Laboratoire d'Ecologie Alpine, UMR-CNRS 5553 (composante d'affectation : UFR Sciences et Montagne)

* Corresponding author (florian.lecorvaisier@vetagro-sup.fr)

Abstract

Cheating is an ubiquitous evolutionary strategy, appearing everywhere throughout the tree of life. Among bacteria, cheating appears mostly through the consumption of public good without participation in their production. Some vaccines, because they specifically target these public goods, may alter the eco-evolutionary dynamics of cheating in bacterial populations of pathogenic species such as *Corynebacterium diphtheriae*, the etiological agent of diphtheria, which produces a public virulence factor. We expand a series of fitness models to assess how the use of vaccines targeting a public good can impact the selective value of its production, alter the ecological dynamics between producers and non-producers, and select for novel phenotypes. Our results show that producers are counter-selected when a vaccine is used but only when the public good is non-mandatory for the growth and survival of the bacteria, and that the presence of non-producers facilitates the eradication of producers. These results advocate for comprehensive studies of the eco-evolutionary consequences of vaccines and illustrate how the competition between non-producers and producers can be useful in the eradication of public virulence factors producers.

Introduction

In ecology and evolutionary biology, cheating can be defined as “a trait that is beneficial to a cheat[er] and costly to a cooperator in terms of inclusive fitness” (Ghoul et al., 2014). This type of behavior is widespread along the tree of life and can emerge at different ecological scales. For example, it has been described between individuals of the same species and sex, such as lekking male frogs satelliting more competitive males (Castellano et al., 2009) between individuals of the same species but opposite sex, such as male spiders deceiving their mates with worthless nuptial gifts (Beydizada et al., 2025) and between individuals of different species, such as cleaner fishes cheating on their clients by feeding on their tissues (Wilson et al., 2014) or non-rewarding female flowers deceiving pollinators by mimicking rewarding male flowers (Castillo et al., 2012).

Cheating necessarily emerges from cooperative behaviors: in the examples above, lekking frogs gather in a chorus to simplify the mating process for every participating male, male spiders

exchange food with a copulation opportunity, cleaner fishes feed on ectoparasites of larger fishes, and pollinators help flowers reproduce while feeding on them. By nature, cheating can thus be differentiated from other interactions such as predation, competition or parasitism (even though intraspecific cheating is sometimes referred to as “intraspecific parasitism”). Cheating has long been questioned in the field of evolutionary biology as an obstacle to the maintenance of cooperative behaviors, while cooperative behaviors themselves have been questioned in the global “selfish-gene” framework (West et al., 2007).

Ghoul et al. (2014) define two families of cheating behavior: interception and manipulation, which we could also refer to as passive and active cheating, respectively. In interception cheating, individuals “hijack” cooperative products or behaviors, while in manipulation cheating cheaters actively exploit cooperative behaviors (for example, by mimicking them) to ensure a gain in fitness at the expense of truly cooperative indi-

viduals. In the examples given above, the behavior of the satellite male frogs would fit within the definition of interception while other behaviors would be classified as manipulation.

Interception is particularly well represented in the domain of bacteria. Many bacterial species or populations produce public goods, i.e., costly molecules which can be beneficial to other cells in the neighborhood of the producer. By nature, production of a public good is a cooperative behavior: all individuals (should) participate in the production of the good and take a part of the common benefit. One of the most studied example of a bacterial public good might be pyoverdine, a siderophore produced by species of the *Pseudomonas* genus (Ghssein & Ezzeddine, 2022). Pyoverdine is mandatory for iron acquisition in multiple environments, and its production is modulated by the availability of iron (Ghssein & Ezzeddine, 2022). There are thus high stakes linked with the production of this molecule and, more broadly, with the production of siderophores. Because of the “public good” property of siderophores, it has been both theorized (Bruce et al., 2017; Lecorvaisier et al., 2024) and shown experimentally (Butaité et al., 2017) that cheaters should and indeed do emerge in siderophore-producing populations of *Pseudomonas*, *Corynebacterium diphtheriae* and other genera and species.

Cheating bacteria that do not produce siderophores can appear in a variety of contexts. In the pathogenic species *P. aeruginosa*, it has been shown that pyoverdine non-producers emerge during lung infections. These non-producers can be classified as cheaters as they maintain the capacity to exploit the pyoverdine produced by cooperative cells. Moreover, it has been shown that the proportion of non-producers increases with time and that the capacity of cheaters to take up the pyoverdine is maintained only until cooperators disappear from the population (Andersen et al., 2015). In natural communities of pseudomonads, it has been shown that the relationship between producers and non-producers is complex, with non-producers developing strategies to exploit the siderophores produced by cooperators, and producers developing

strategies to repress cheating behaviors, much like what the Red Queen hypothesis describes (Bruce et al., 2017; Butaité et al., 2017).

As any evolutionary strategy, cheating is complex. On one hand, and as exemplified above with pyoverdine cheaters, it may emerge or disappear due to changes in the environment (e.g., change in resources, in population density...) and may not always be expected or predictable (Ghoul et al., 2014). On the other hand, we live in an ever-changing world where global warming, globalization, antibiotics... create new environments and life conditions for millions of species. All these phenomena may have an impact on the evolution of cheating as a behavior and cheaters as a population. In the present study, we focus on one global change: vaccination. Vaccines against many diseases became widespread during the second half of the 20th century and lead to evolutionary consequences such as the emergence of vaccine-escape strains of the hepatitis B virus (Santos et al., 2017; Wang et al., 2017), the emergence of hypervirulent strains of the Marek’s disease virus (Gimeno, 2008), and multiple important changes in the genotype and phenotype of circulating strains of *Bordetella pertussis*, the etiological agent of whooping cough (Lefrancq et al., 2022).

We hypothesize that vaccines specifically targeting public goods, such as modern diphtheria vaccines, should alter the dynamics between cooperator and cheater phenotypes. To investigate this hypothesis, we expand a theoretical model of competition between strains of a bacterium producing a public good. Understanding how vaccination may alter this competition is of great importance as public goods can also be virulence factors or linked to virulence factors, as are the diphtheria toxin of *C. diphtheriae* (Tiwari & Wharton, 2012) or the pyoverdine of *P. aeruginosa* (Buckling et al., 2007).

Model & Results

Bruce et al. (2017) proposed a mathematical model describing the competition dynamics between two types of cells (or phenotypes) in a population of bacteria. The first type is called “cooperator cell”, named like this because it pro-

duces a public good necessary for the growth of any cell of the population. The second type is called “cheater cell” because it does not produce the public good but is able to use the good produced by cooperator cells. Their model defines the fitness of the cell as a function of the energetic cost of producing the good, q , among other parameters. If costly, producing the public good is also beneficial to the cell, as it is mandatory for the reproduction and survival of the cell.

This model describes the ecology and evolution of an environmental bacteria, *Pseudomonas fluorescens*, but it can be applied to other biological systems. In the present work, we generalize the model developed by Bruce et al. (2017) while simplifying some aspects, and apply its study to the case of pathogenic bacteria with different phenotypes, noted i and considered here through the variability in the production of the public good.

The fitness of any i -phenotype cell can be expressed as

$$W_i = C_i (B_i + B_j)^\alpha, \quad (1)$$

where C_i is the cost of producing goods (public or private) for cell i and $(B_i + B_j)^\alpha$ is the benefit for cell i , α being a shape parameter. The benefit is divided in two parts: the benefit linked to the individual production of the i -phenotype cell production (B_i) and the benefit linked to the public good production from other cells, from the same or different phenotype (B_j).

The cost of the good production is

$$C_i = 1 - q_i - g, \quad (2)$$

where $0 \leq q_i < 1$ is the production of the public good for an i -phenotype cell and $0 \leq g < 1$ is the production of other (private) goods, considered equal among cells. We consider that $q_i + g < 1$ to avoid the cost of producing the different goods to reach one.

The benefit for an i -phenotype cell derived from its own production is

$$B_i = (1 - \lambda)(1 - \eta)q_i + g, \quad (3)$$

where λ is the fraction of the public good production that is shared with other cells in the

population and η is the efficacy of an (imperfect) vaccine targeting the public good. If $\lambda = 0$ then the good is not shared at all and that it is in reality a private good. Thus, we posit $\lambda > 0$.

The benefit for an i -phenotype cell derived from the production of other cells is

$$B_j = \lambda(1 - \eta) \sum_j x_j q_j \quad (4)$$

where x_j is the fraction of j -type cells in the population and q_j is the good production by j -phenotype cells (including other i -phenotype cells). In the following of this work, we will call B_i the “private benefit” and B_j the “public benefit”.

There are three main differences between this model and the one proposed by Bruce et al. (2017). The first one is that their model takes into account a degree of variability in the ability of cells to exploit public goods produced by other cells, which we neglect here. The second one is that their model considers the public good to be essential for the fitness of the cells, while in our model the fitness of an i -phenotype cell can be positive as long as $g > 0$ and $1 - q_i - g > 0$. Finally, the third and most important difference is that our model considers the use of a vaccine targeting the public good.

Equation 1 can be modified to illustrate a variety of ecological situations with different degrees of complexity and biological realism. The simplest situation is to consider an homogeneous population where all cells are of the same type ($j = i$) and thus share the same cost of producing the public good ($q_i = q_j = q_1$). In this case, each cell has the same fitness, independent of the fraction of the public good shared with other cells (λ).

This fitness is

$$W_1 = C_1 (B_i + B_j)^\alpha, \quad (5)$$

where $C_1 = 1 - q_1 - g$ and $B_i + B_j = (1 - \eta)q_1 + g$.

We observe that the higher the vaccine efficacy, the lower the fitness of the cells (Figure 1). This is easily explained considering that the vaccine removes the benefit of producing the public good

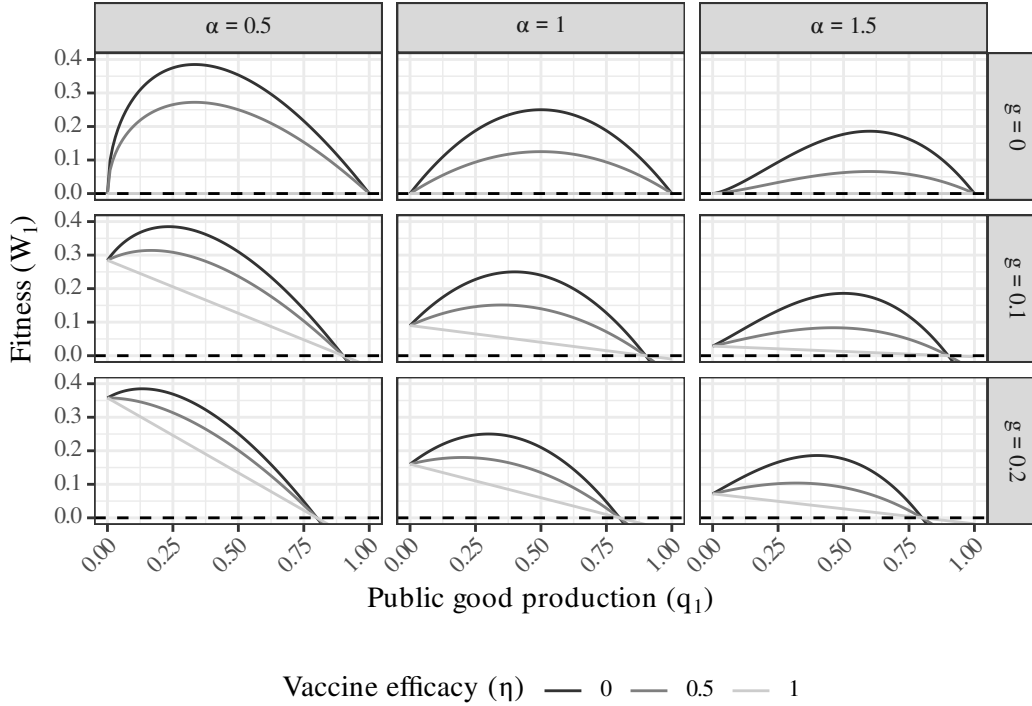


Figure 1: Fitness of the cell type 1 (W_1) as a function of public good production (q_1) for different values of vaccine efficacy (η), private good production (g) and shape parameter (α). The dashed lines indicate the lowest natural boundary for W_1 .

without diminishing the cost of production. Interestingly, we observe that, except when $\eta = 1$ and it is linear, the relation between the fitness, W_1 and the production of the public cost, q_1 , follows a concave curve. This means that there exists an intermediate optimal value for the production of the public good that graphically appears to depend on the values of α , g and η .

Let q_1^* be the optimal production of the public good, i.e., the value of q_1 maximizing the fitness of the cells in this scenario. In a first, naive interpretation, this value could be thought as the one eventually reached by the clonal population because of natural selection (but see infra). It can be expressed as

$$q_1^* = \frac{\alpha}{\alpha + 1} - g \frac{\alpha(1 - \eta) + 1}{(1 - \eta)(\alpha + 1)}. \quad (6)$$

Equation 6 confirms the graphical observation from Figure 1 that the optimal public good production depends on the vaccine efficacy, η , the production of the private good, g , and the shape parameter, α . When $\eta = 1$, the second denominator in Equation 6 goes to zero. This corresponds

to a situation in which the vaccine is perfect and the benefit from producing the public good is removed from Equation 5.

We observe in Equation 6 that it is possible that $q_1^* < 0$. Indeed, the left term is always lower than one because $\alpha > 0$ and the right term is always positive because $0 \leq g \leq 1$ and $0 \leq \eta \leq 1$; and the right term converges toward infinity when η converges toward one. This implies that production of the public good can be counter-selected under certain circumstances.

This is graphically confirmed in Figure 2, hinting to the existence of a vaccine efficacy threshold above which counter-selection occurs. Figure 2 also shows that the vaccine efficacy only impacts the optimal public good production when there is some form of private good production (i.e., $g \neq 0$).

Let η'_1 be the vaccine efficacy threshold above which the production of the public good should be counter-selected, i.e., the value such that $q_1^*(\eta = \eta'_1) = 0$. This value is

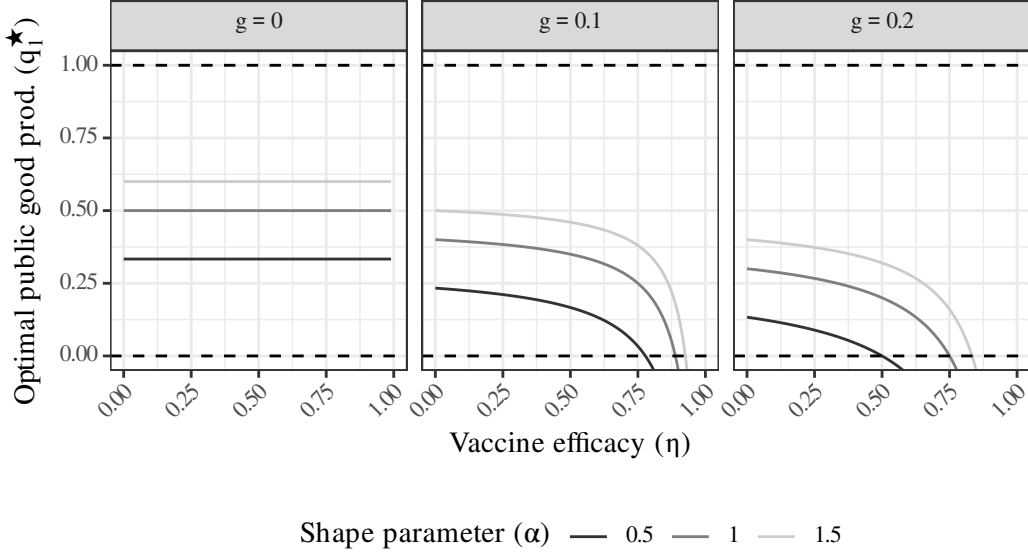


Figure 2: Optimal public good production (q_1^*) as a function of vaccine efficacy (η) for different values of shape parameter (α) and private good production (g). The dashed lines indicate the natural boundaries of q_1^* .

$$\eta'_1 = 1 - \frac{g}{\alpha(1-g)}, \quad (7)$$

and we can show that for all $\eta > \eta'_1$, $q_1^* < 0$. This finding is particularly interesting because it shows that the private good production plays an important role on the value of this vaccine efficacy threshold. We observe that the higher the private good production, the lowest the vaccine efficacy threshold (Figure 3).

Interestingly, we can also observe a certain threshold in the private good production beyond which the production of the public good is counter-selected whatever the vaccine efficacy (i.e., $\eta'_1 \leq 0$). This threshold is

$$g'_1 = \frac{\alpha}{\alpha + 1}. \quad (8)$$

Until now, we considered the simplest possible model where the population was composed of

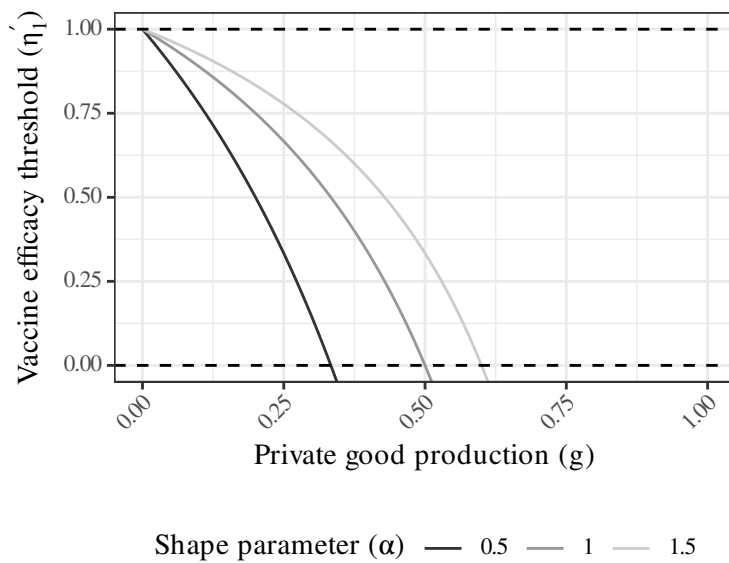


Figure 3: Vaccine efficacy threshold (η'_1) as a function of private good production (g) for different values of the shape parameter (α). The dashed lines indicate the natural boundaries of η'_1 .

clonal cells. In the following part, we consider a dimorphic population. The first phenotype, which we call “cooperator” or 2.1-type, produces the public good with a level $q_{2.1} > 0$. The second phenotype, which we call “cheater” or 2.2-type, does not produce the public good ($q_{2.2} = 0$) but, as hinted in Equation 1, it can profit from public goods produced by cooperator cells. The fitness of the cooperator phenotype is

$$W_{2.1} = C_{2.1}(B_{2.1} + B_j)^\alpha, \quad (9)$$

and the fitness of the cheater phenotype is

$$W_{2.2} = C_{2.2}(B_{2.2} + B_j)^\alpha. \quad (10)$$

The cost for any cooperator cell is

$$C_{2.1} = 1 - q_{2.1} - g, \quad (11)$$

while the cost for any cheater cell is

$$C_{2.2} = 1 - g. \quad (12)$$

Thus, because $q_{2.1} > 0$, we know that $C_{2.2} < C_{2.1}$, meaning that cheater cells have a lower cost than cooperator cells.

On the other hand, each cooperator cell has a personal benefit

$$B_{2.1} = (1 - \lambda)(1 - \eta)q_{2.1} + g, \quad (13)$$

and each cheater cell has a personal benefit

$$B_{2.2} = g, \quad (14)$$

while each cell in the population has a public benefit

$$B_j = \lambda(1 - \eta)x_{2.1}q_{2.1}. \quad (15)$$

where $x_{2.1}$ is the proportion of cooperator cells in the population. We note that, as stated earlier and contrarily to the original model by Bruce et al. (2017), cheater cells can have a positive fitness in the absence of cooperator cells (i.e., when $x_{2.1} = 0$) as long as the production of the private good is not null (i.e., $g > 0$).

Depending on the parameters values, and because the proportion of cooperator cells is by nature not static, different outcomes may emerge for this scenario. It is possible that the fitness of the cooperator phenotype exceed the fitness of

the cheater phenotype whatever the proportion of cooperator cells (e.g., Figure 4, top-left panel). In this case, the proportion of cooperator cells should gradually increase, leading the cheater phenotype to extinction (Figure 5). Another possible outcome is the fitness of the cheater phenotype exceeding the fitness of the cooperator phenotype whatever the proportion of cooperator cells (e.g., Figure 4, bottom-left panel). In this case, the proportion of cooperator cells should gradually decrease, leading the cooperator phenotype to extinction (Figure 5). Finally, in the third possible outcome, the fitness of the cooperator phenotype may be higher or lower than the fitness of the cheater phenotype depending on the proportion of cooperator cells (e.g., Figure 4, middle-left panel). In this case, the proportion of cooperator cells should converge toward a value where $W_{2.1} = W_{2.2}$ and both phenotypes should coexist (Figure 5).

This phenomenon emerges because of the nature of the interaction of the two different phenotypes. Equation 9 and Equation 10 show that the fitness of both phenotypes increases along with the relative prevalence of cooperator cells, $x_{2.1}$. Moreover, because it does not bear any cost of public good production, the fitness of cheater cells, $W_{2.2}$, increases faster than the fitness of cooperator cells, $W_{2.1}$, when $x_{2.1}$ increases (Figure 4, all panels). However, if $W_{2.2} > W_{2.1}$, then the relative prevalence of cooperator cells should decrease because of the competitive advantage of cheater cells, leading to a decrease in the fitness of the cheater phenotype. Therefore, as stated above, the proportion of cooperator cells should converge toward an optimal, stable value for which $W_{2.1} = W_{2.2}$. This value is given in Equation 16.

We observe that the numerator of Equation 16 can fall below zero, which would result in $x_{2.1}^*$ to also fall below zero. This outcome corresponds to the situation exposed earlier where the cooperator phenotype goes extinct. We observe that the denominator is zero if $\eta = 1$ or $q_{2.1} = 0$. In these situations, the production is either null or nullified by the vaccine, leading automatically the cooperator phenotype to extinction, and $x_{2.1}^*$ does not exist.

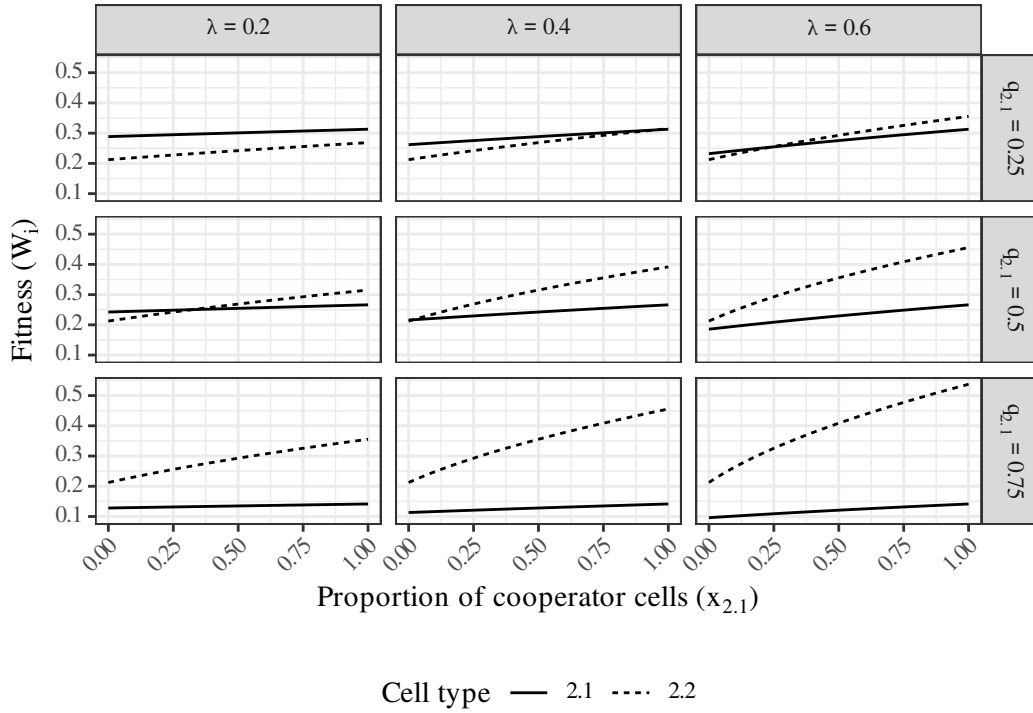


Figure 4: Fitness of the cell types 2.1 ($W_{2,1}$) and 2.2 ($W_{2,2}$) as a function of the proportion of cooperator cells ($x_{2,1}$) for different values of the fraction of the public good that is shared (λ) and public good production ($q_{2,1}$). Other parameter values are $\alpha = 0.5$, $\eta = 0.4$ and $g = 0.05$.

In the special case where $g = 0$ (i.e., the fitness is completely conditioned by the production of the public good) we can notice that it is not theoretically possible for the cooperator phenotype

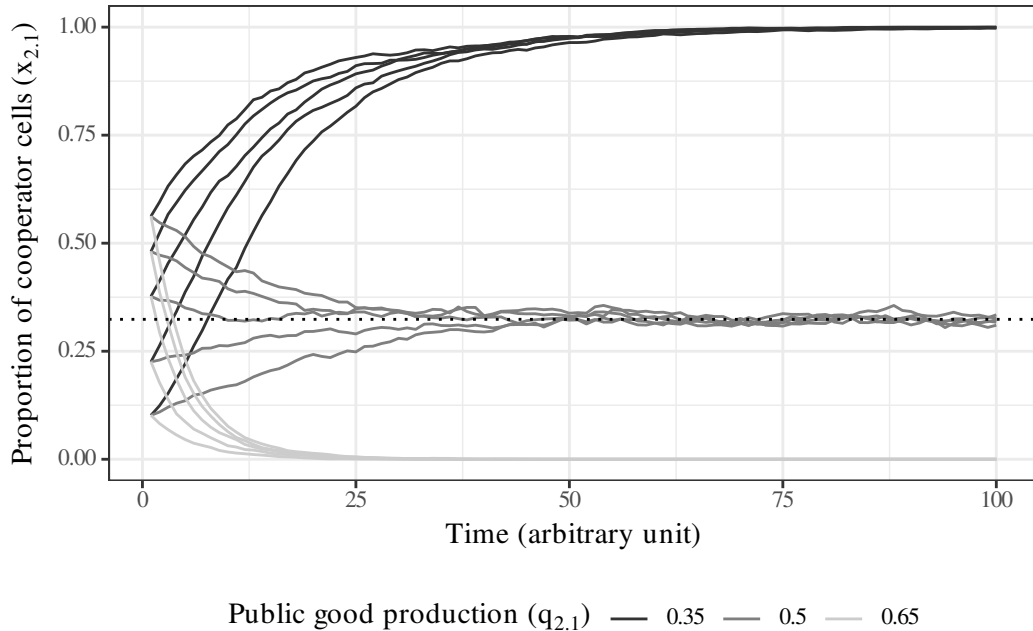


Figure 5: Change in the proportion of cooperator cells ($x_{2,1}$) with time for different values of public good production ($q_{2,1}$). Other parameters values are $\alpha = 0.5$, $\eta = 0.4$, $g = 0.05$ and $\lambda = 0.2$. The dotted line indicates the converging value of $x_{2,1}$ for $q_{2,1} = 0.5$ according to Equation 16. For details on the simulator, see the Supplementary material.

to go extinct because of competitive pressure, except if $\lambda = 1$ (the public good is completely shared), or in one of the two situations described above: $\eta = 1$ (the vaccine “perfectly” blocks the fitness) or $q_{2,1} = 0$ (no public good is produced). Note that in any of these three possible cases the cheater phenotype should go extinct as well since its fitness relies entirely on the existence of the cooperator phenotype when $g = 0$. Reciprocally, it is possible that the numerator exceeds the denominator, which would result in $x_{2,1}^*$ to go beyond one. This outcome corresponds to the situation where the cheater phenotype goes extinct.

Globally, we can observe that the proportion of cooperator cells decreases when the production of the public good increases, even when there is no production of a private good (Figure 6). It also

appears that the larger the fraction of the public good that is shared among the population, the easier it is for the cooperator phenotype to be maintained (Figure 6, columns); and the higher the vaccine efficacy, the easier it is for the cooperator phenotype to go extinct (Figure 6, rows). Also, we observe that the higher the private good production, the lowest the optimal proportion of cooperator cells (Figure 6, colors).

As we did for the first model, it is interesting to investigate the vaccine efficacy threshold, i.e., the value of η such that the cooperator phenotype should go extinct. We consider that $x_{2,1}$ fluctuates way faster than $q_{2,1}$ (because, in our model, a change in $q_{2,1}$ implies a mutation, while a change in $x_{2,1}$ does not). Thus, we will consider the vaccine efficacy threshold as the value of η for which $x_{2,1}^* = 0$. This value, which we call $\eta'_{2,1}$, is given

$$x_{2,1}^* = \frac{(1 - q_{2,1} - g)^{\frac{1}{\alpha}} ((1 - \lambda)(1 - \eta)q_{2,1} + g) - (1 - g)^{\frac{1}{\alpha}} g}{\lambda(1 - \eta) \left((1 - g)^{\frac{1}{\alpha}} - (1 - q_{2,1} - g)^{\frac{1}{\alpha}} \right) q_{2,1}} \quad (16)$$

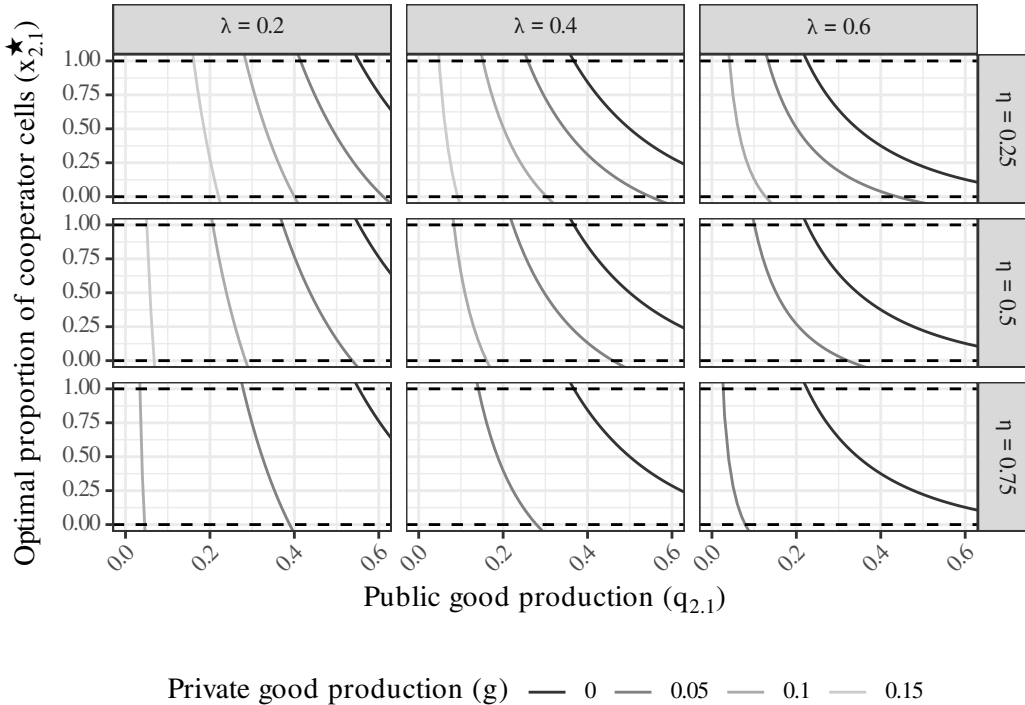


Figure 6: Optimal proportion of cooperator cells ($x_{2,1}^*$) as a function of the public good production ($q_{2,1}$) for different values of the private good production (g), fraction of the good that is shared (λ) and vaccine efficacy (η). The shape parameter value is $\alpha = 0.5$. The dashed lines indicate the natural boundaries of $x_{2,1}^*$.

in Equation 17. In this formula, the denominator goes to zero if $q_{2,1} = 0$ or $\lambda = 1$. The first situation implies that no public good is produced, and thus $\eta'_{2,1}$ does not exist. The second situation implies that the good is perfectly public. In this case, the production of the public good is always counter-selected and $\eta'_{2,1}$ does not exist either.

We observe that the vaccine efficacy threshold decreases when the public good production increases, showing how the selective pressure created by the vaccine is stronger when the cell relies heavily on the production of the public good for its fitness (Figure 7). We can also observe that the vaccine efficacy threshold is lower when the proportion of the public good that is shared is high, illustrating how competition between producers and cheaters for access to the public good acts synergically with the vaccine against producers (Figure 7, columns). Similarly,

it decreases when the private good production increases, illustrating the selective advantage of producing a private good rather than a public one when the public good is targeted by a highly efficient vaccine (Figure 7, rows).

The scenarios presented above, while mentioning mutations and changes in frequency, are really static in nature. They do not take into account the adaptive dynamics of the population. Let's now consider a homogeneous population, much like what was proposed in the first scenario. The fitness of any cell in this scenario is given in Equation 5 but let's name the fitness $W_{3,1}$ and the public good production $q_{3,1}$ for the sake of clarity. Let's now consider a mutant cell, with a production of the public good $q_{3,2}$. If we consider a very large population such that $x_{3,1} = 1$ (where $x_{3,1}$ is the proportion of cells with the wild phenotype) when the mutant cell emerges

$$\eta'_{2,1} = 1 - \frac{\left((1-g)^{\frac{1}{\alpha}} - (1-q_{2,1}-g)^{\frac{1}{\alpha}} \right) g}{(1-\lambda)(1-q_{2,1}-g)^{\frac{1}{\alpha}} q_{2,1}} \quad (17)$$

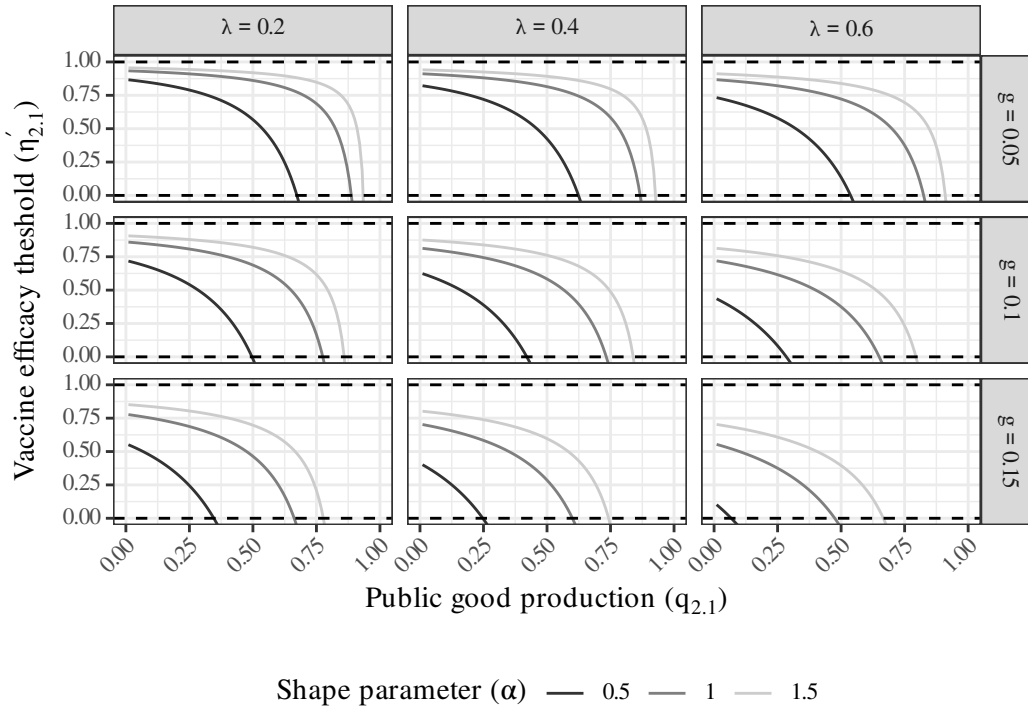


Figure 7: Vaccine efficacy threshold ($\eta'_{2,1}$) as a function of the public good production ($q_{2,1}$) for different values of the shape parameter (α), fraction of the good that is shared (λ) and private good production (g). The dashed lines indicate the natural boundaries of $\eta'_{2,1}$.

in the population, the fitness of the mutant cell is given in Equation 18.

The mutant cell can multiply if its fitness is higher than the fitness of resident cells, i.e., if $W_{3.2} > W_{3.1}$ or, in other words, if its invasion fitness is positive, i.e., if $\omega_{3.2} > 0$ with $\omega_{3.2} = W_{3.2} - W_{3.1}$. We can observe that there are varieties of situations where the mutant strain can invade and replace the resident strain population (Figure 8, dark grey areas) and varieties of situations where it can not (Figure 8, light grey areas). In the first situation, the proportion of mutant cells, $x_{3.2}$, increases and eventually reaches one, while the proportion of resident cells, $x_{3.1}$, decreases and eventually reaches zero. In the second situation, $x_{3.2}$ stays zero and $x_{3.1}$ stays one.

Interestingly, if we reciprocally calculate the invasion fitness of resident strains, $\omega_{3.1}$, we discover that there are also $q_{3.1}$ and $q_{3.2}$ values combinations where both phenotypes can invade each other, leading to coexistence (Figure 8, medium gray areas). This implies that $x_{3.1}$ will

decrease but not reach zero while $x_{3.2}$ will increase but not reach one, contrarily to the situations shown in the dark grey areas. In other words, in light grey areas, we have $\omega_{3.1} > 0$ and $\omega_{3.2} \leq 0$; in dark grey areas, we have $\omega_{3.1} \leq 0$ and $\omega_{3.2} > 0$, and in medium gray areas we have $\omega_{3.1} > 0$ and $\omega_{3.2} > 0$.

Using an extension of Equation 16 for which “cheater” cells have a public good production $q_{2.2} > 0$, we observe that the dark, light and medium grey area on Figure 8 correspond to $x_{2.1}^* < 0$, $x_{2.1}^* > 1$ and $0 < x_{2.1}^* < 1$, respectively (not shown).

We can show that there exists a singular public good production value, $q_{3.1}^*$, that should ultimately be reached when a long enough time has been spent and mutations occur altering the public good production. A phenotype producing such an amount of public good cannot be invaded and is thus an evolutionary stable strategy (ESS). This value is

$$W_{3.2} = (1 - q_{3.2} - g)((1 - \lambda)(1 - \eta)q_{3.2} + \lambda(1 - \eta)q_{3.1} + g)^\alpha \quad (18)$$

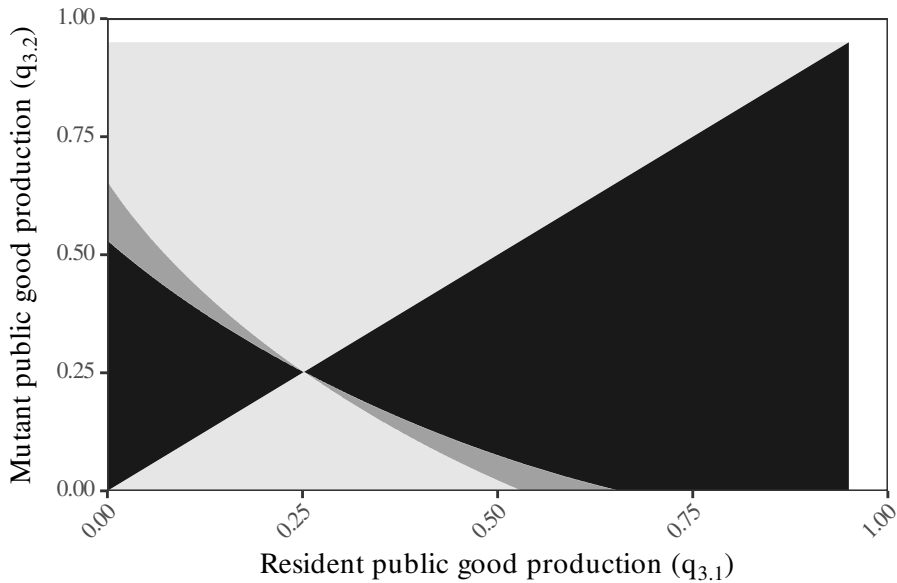


Figure 8: Pairwise invasibility plot. Dark grey areas indicate a positive invasion fitness while light grey areas indicate a negative invasion fitness. Medium gray areas indicate mutual invasion and thus coexistence. White areas indicate undefined space ($q_{(\cdot)} > 1 - g$). Other parameters values are $\alpha = 0.5$, $\eta = 0.2$, $\lambda = 0.1$ and $g = 0.05$.

$$q_{3.1}^* = \frac{\alpha}{\alpha + \frac{1}{1-\lambda}} - g \frac{\alpha(1-\eta) + \frac{1}{1-\lambda}}{(1-\eta)(\alpha + \frac{1}{1-\lambda})}. \quad (19)$$

Interestingly, we see that the higher the shared portion of the public good (λ), the lowest the value of $q_{3.1}^*$. Reciprocally, the lower the value of λ , the highest the value of $q_{3.1}^*$ and, for $\lambda = 0$ we have $q_{3.1}^* = q_1^*$, i.e., the ESS matches the optimal strategy. This means that, for $\lambda \neq 0$, the ESS is less than optimal (Figure 9B). In the end, a clonal population should appear with a lower fitness than the maximal one it could theoretically achieve (Figure 9C).

Note that, on Figure 9, new mutants appear even when the population is not clonal (Figure 9A), i.e., the fitness of mutants is not equal to the one

formulated by Equation 18 but to the one given by Equation 1. Moreover, the “final” public good production and clonal fitness are different than the theoretical values because of the small population size and high mutation rate, leading to drift (see Supplementary material).

Let $\eta'_{3.1}$ be the vaccine efficacy threshold above which the evolutionary stable public good production is equal to zero, i.e., the value such that $q_{3.1}^*(\eta = \eta'_{3.1}) = 0$. This value is

$$\eta'_{3.1} = 1 - \frac{g}{\alpha(1-\lambda)(1-g)}, \quad (20)$$

and we can show that for all $\eta > \eta'_{3.1}$, $q_{3.1}^* < 0$. This formula is similar to Equation 7 with the only difference being the addition of the propor-

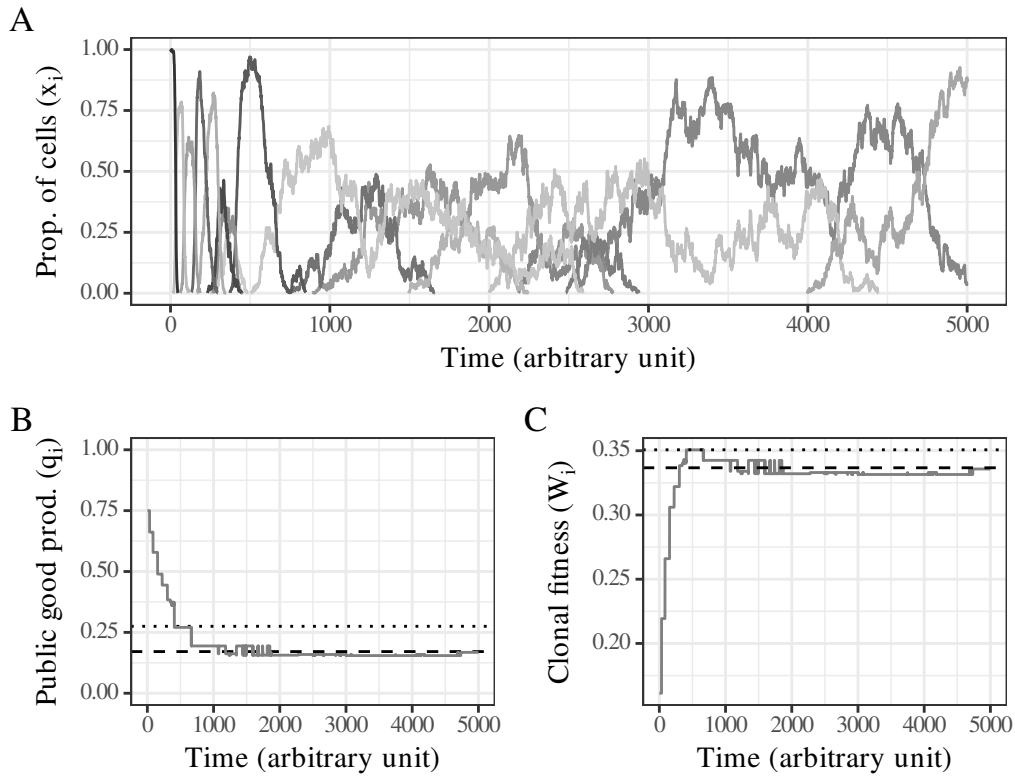


Figure 9: Evolution of the public good production when mutations occur. **(A)** Proportion of cells of different phenotypes (x_i , i as colors) as a function of time. Only phenotypes becoming dominant are shown to increase readability. **(B)** Public good production of the dominant phenotype (q_i) as a function of time. The dotted line represents the optimal public good production according to Equation 6 and the dashed line represents the evolutionary stable public good production according to Equation 19. **(C)** Fitness of the dominant phenotype (W_i) if it was in a clonal population. The dotted line represents the fitness with the optimal public good production and the dashed line represents the fitness with the evolutionary stable public good production (Equation 1). Other parameters values are $\alpha = 0.5$, $\eta = 0.2$, $\lambda = 0.4$ and $g = 0.05$. For details on the simulator, see the Supplementary material.

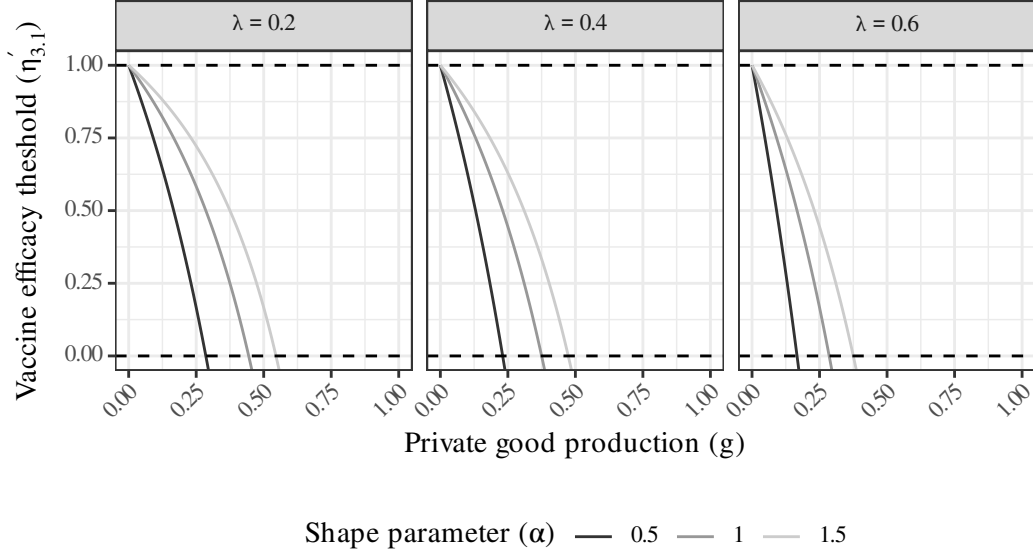


Figure 10: Vaccine efficacy threshold ($\eta'_{3,1}$) as a function of the private good production (g) for different values of the shape parameter (α) and fraction of the good that is shared (λ). The dashed lines indicate the natural boundaries of $\eta'_{3,1}$.

tion of the public good that is shared with other cells (λ) in the formula. We observe that the higher this value, the lower the vaccine efficacy threshold (Figure 10). Also, and similarly to what was shown earlier, we observe that the highest the production of the private good, the lowest the vaccine threshold. As before, we can show that there is a private good production threshold above which the public good production is counter-selected whatever the vaccine efficacy.

This value is

$$g'_{3,1} = \frac{(1-\lambda)\alpha}{(1-\lambda)\alpha + 1}. \quad (21)$$

It implies that the higher the value of λ , i.e., the more the public good is shared among other cells, the lower the private good production needed for the public good production to be counter-selected.

Discussion

The first model we presented, which we may call the “one-strain” scenario and that we formulated with Equation 5, may be plausible on a short time scale. At the beginning of an infection, an individual may be infected only by one variant from a bacterial population because of the bottleneck applied when a pathogen jumps from one

host to the next (De Ste Croix et al., 2020; Zwart & Elena, 2015) or because the previous host was already carrying a clonal population of bacteria, for example because of the use of an antibiotics therapy (McVicker et al., 2014). We showed with this model that the use of a vaccine targeting the public good should decrease the fitness of the cells, a finding that is of particular interest from a medical point of view. First, because a decrease in the fitness should lead to a decrease in the multiplication rate and thus a decrease in the bacterial load, which is correlated to morbidity and mortality in many pathogenic systems such as *Neisseria meningitidis* (Darton et al., 2009), *Streptococcus pneumoniae* (Rello et al., 2009) or *Mycobacterium tuberculosis* (Pasipanodya et al., 2015) infections. Second, because the decrease in fitness can be so high that the production of the public good may be counter-selected. This is particularly interesting if the public good targeted by the vaccine is a virulent factor, like the diphtheria toxin is targeted by modern vaccines against *Corynebacterium diphtheriae* (Pappenheimer Jr., 1984).

We also showed with this model that vaccines create novel environmental conditions under which the most efficient phenotype shifts. Interestingly, this finding only holds when there

exists an alternative metabolic pathway making the production of the vaccine-targeted public good non-mandatory for the multiplication or survival of the cells. This illustrates how vaccines alter the selective pressures weighting on (pathogenic) bacteria, something largely described in the literature with species such as *Streptococcus pneumoniae* (Brueggemann et al., 2007) and *Bordetella pertussis* (Lecorvaisier, 2024; Lefrancq et al., 2022).

The second model, which we may call the “cooperator-cheater” scenario and that we formulated with Equation 9 and Equation 10, may be more plausible than the first one at an intermediate time scale, when a mutation leading to the appearance of a phenotype not producing the public good had time to emerge and increase in frequency. We showed with this model that, in the absence of a vaccine, the relationship between producers and cheaters is driven by the production of the different types of goods and the accessibility of public goods. Intuitively, one could think that producing a public good in the presence of cheaters while a alternative private metabolic pathway exists should be counter-selected, and that cooperators should ultimately vanish with the capacity of producing said public good (Black Queen hypothesis). This apparent problem finds its solution if we consider that public goods are only partly public and thus can that cooperators cells better exploit there own public good production than other cells, improving the global fitness of cells producing both private and (partially) public goods (Bruce et al., 2017; Lerch et al., 2022).

When a vaccine is used, the environmental conditions shift and the advantage given to producers diminishes, increasing the frequency of the cheater phenotype. Nevertheless, for producers to completely vanish, and similarly to what was concluded with the one-strain model, it is necessary that an alternative metabolic exists to compensate for the loss of the public good production function in the population.

The first and second models have similar conclusions in showing that increasing the vaccine efficacy leads to a decrease in the fitness of cells

producing the public good. But the cooperator-cheater model gives us a new insight, as we saw that the decrease in the fitness and thus frequency of producers was amplified by the presence of the competitive, cheater phenotype. In the case where the public good is a virulence factor, this finding implies that designing vaccines specifically targeting such virulence-related public goods could act synergically with the competition by cheater cells to lead to the eradication of pathogenic cells, something already found in a between-hosts model of transmission of diphtheria (Lecorvaisier et al., 2024).

The third model, which we may call the “invasion” scenario and that we formulated with Equation 18, can be plausible at a long time scale, when multiple mutations have time to appear. This model is again interesting when compared to the precedent ones. The one-strain model gave us the optimal (in term of fitness) public good production. This model shows that, in the long run, natural selection, through competition to the access of public goods, favors a less-than-optimal public good production. As the cooperator-cooperator model illustrated, this model shows that coexistence between high- and low-producing cells is possible, but the population should ultimately converge toward a clonal phenotype.

When looking at the effect of a vaccine, we discovered that the higher the vaccine efficacy, the lowest the ESS of public good production. For really high values of the vaccine efficacy, it is even possible that the ESS is to stop producing the public good. In this case, vaccination appears as a viable strategy to drive the evolution of pathogens toward non-production of a public good. As discussed earlier, this is particularly interesting in the case where the public good is a virulence factor.

Our work shows that cheating may emerge as a medium-term strategy without being evolutionary stable. From a theoretical ecology point of view, this means that cheaters should eventually disappear from the population. Nevertheless, in real-life settings, environmental conditions are so stochastic and perturbations occurs at such high rates that it is unlikely that a population

eventually reaches the theoretical ESS. Moreover, in this model, the ESS relies on parameter values that may change over time, such as the vaccine efficacy, which may change one way by the selection of novel bacterial alleles diminishing the efficacy, and the other way by the deployment of new vaccines with a higher efficacy. This implies that the evolution of pathogens following the use of vaccines should be carefully monitored and studied to evaluate the effects of this selective pressure.

As any modelling work, our study has some flaws and limits. One of these is that the public good production is considered as constant, while in real biological settings the production may fluctuate with time and the resource availability. For example, the diphtheria toxin production in *C. diphtheriae* is conditioned by the iron availability in the host (Parveen et al., 2019).

Another important limit is that our analysis focuses on the within-host competitive dynamics between strains, without considering the between-hosts dynamics and the competition for new hosts. It would be interesting to study how selective pressure at the within-host scale could alter the between-hosts spread of novel strains in a vaccination context. For example, we hypothesize that the population heterogeneity in the vaccine status can strongly alter the competitive dynamics between multiple strains.

Despite these limits, our model has strong implications for vaccine development and vaccination strategies. We show that vaccine strategies have complex evolutive outcomes that must be studied before being deployed, and that ecological relationships between organisms can be used in the fight against pathogenic strains or species.

CRediT authorship

Florian Lecorvaisier: Conceptualization, Investigation, Methodology, Software, Visualization, Writing - original draft **Thomas L. P. Martin:** Investigation, Methodology, Formal analysis, Writing - review & editing.

Supplementary information

Proofs of Equation 6, Equation 7, Equation 16, Equation 19 and Equation 20 are available in the Supplementary material of this article, as well as the protocols used for the simulators illustrated in Figure 5 and Figure 9. The code to produce all the figures is available at <https://github.com/FloLecorvaisier/cheating-vaccine>.

Bibliography

- Andersen, S. B., Marvig, R. L., Molin, S., Krogh, J., & Griffin, A. S. (2015). Long-term social dynamics drive loss of function in pathogenic bacteria. *Proceedings of the National Academy of Sciences*, *112*(34), 10756–10761. <https://doi.org/10.1073/pnas.1508324112>
- Beydzada, N. I., Martini, S., Beyer, M., & Tunj, C. (2025). Who Is Likely to Cheat? Linking Personality to Worthless Gift Production in a Spider. *Ethology*, *131*(12), 313–320. <https://doi.org/10.1038/s41467-017-00509-4>
- Bruce, J. B., Cooper, G. A., Chabas, H., West, S. A., & Griffin, A. S. (2017). Cheating and resistance to cheating in natural populations of the bacterium *Pseudomonas fluorescens*. *Evolution*, *71*(10), 2484–2495. <https://doi.org/10.1111/evo.13328>
- Brueggemann, A. B., Pai, R., Crook, D. W., & Beall, B. (2007). Vaccine Escape Recombinants Emerge after Pneumococcal Vaccination in the United States. *PLOS Pathogens*, *3*(11), e168. <https://doi.org/10.1371/journal.ppat.0030168>
- Buckling, A., Harrison, F., Vos, M., Brockhurst, M. A., Gardner, A., West, S. A., & Griffin, A. (2007). Siderophore-mediated cooperation and virulence in *Pseudomonas aeruginosa*. *FEMS Microbiology Ecology*, *62*(2), 135–141. <https://doi.org/10.1111/j.1574-6941.2007.00388.x>
- Butaitė, E., Baumgartner, M., Wyder, S., & Kümmerli, R. (2017). Siderophore cheating and cheating resistance shape competition for iron in soil and freshwater *Pseudomonas* communities. *Nature Commu-*

- nications*, 8(1), 414. <https://doi.org/10.1038/s41467-017-00509-4>
- Castellano, S., Marconi, V., Zanollo, V., & Berto, G. (2009). Alternative mating tactics in the Italian treefrog, *Hyla intermedia*. *Behavioral Ecology and Sociobiology*, 63(8), 1109–1118. <https://doi.org/10.1007/s00265-009-0756-z>
- Castillo, R. A., Caballero, H., Boege, K., Fornoni, J., & Dominguez, C. A. (2012). How to cheat when you cannot lie? Deceit pollination in *Begonia gracilis*. *Oecologia*, 169(3), 773–782. <https://doi.org/10.1007/s00442-012-2250-y>
- Darton, T., Guiver, M., Naylor, S., Jack, D. L., Kaczmarek, E. B., Borrow, R., & Read, R. C. (2009). Severity of Meningococcal Disease Associated with Genomic Bacterial Load. *Clinical Infectious Diseases*, 48(5), 587–594. <https://doi.org/10.1086/596707>
- De Ste Croix, M., Holmes, J., Wanford, J. J., Moxon, E. R., Oggioni, M. R., & Bayliss, C. D. (2020). Selective and non-selective bottlenecks as drivers of the evolution of hypermutable bacterial loci. *Molecular Microbiology*, 113(3), 672–681. <https://doi.org/10.1111/mmi.14453>
- Ghoul, M., Griffin, A. S., & West, S. A. (2014). TOWARD AN EVOLUTIONARY DEFINITION OF CHEATING. *Evolution*, 68(2), 318–331. <https://doi.org/10.1111/evo.12266>
- Ghssein, G., & Ezzeddine, Z. (2022). A Review of *Pseudomonas aeruginosa* Metallophores: Pyoverdine, Pyochelin and Pseudopaline. *Biology*, 11(12), 1711. <https://doi.org/10.3390/biology11121711>
- Gimeno, I. M. (2008). Marek's disease vaccines: A solution for today but a worry for tomorrow?. *Vaccine*, 26(s3), C31–C41. <https://doi.org/10.1016/j.vaccine.2008.04.009>
- Lecorvaisier, F. (2024). Impact de la vaccination sur l'évolution de *Bordetella pertussis*. *Médecine/sciences*, 40(2), 161–166. <https://doi.org/10.1051/medsci/2023219>
- Lecorvaisier, F., Pontier, D., Soubeyrand, B., & Fouchet, D. (2024). Using a dynamical model to study the impact of a toxoid vaccine on the evolution of a bacterium: The example of diphtheria. *Ecological Modelling*, 487, 110569. <https://doi.org/10.1016/j.ecolmodel.2023.110569>
- Lefrancq, N., Bouchez, V., Fernandes, N., Barkoff, A.-M., Bosch, T., Dalby, T., Åkerlund, T., Darenberg, J., Fabianova, K., Vestrheim, D. F., Fry, N. K., González-López, J. J., Gullsby, K., Habington, A., He, Q., Litt, D., Martini, H., Piérard, D., Stefanelli, P., ... Brisse, S. (2022). Global spatial dynamics and vaccine-induced fitness changes of *Bordetella pertussis*. *Science Translational Medicine*, 14(642), eabn3253. <https://doi.org/10.1126/scitranslmed.abn3253>
- Lerch, B. A., Smith, D. A., Koffel, T., Bagby, S. C., & Abbott, K. C. (2022). How public can public goods be? Environmental context shapes the evolutionary ecology of partially private goods. *PLOS Computational Biology*, 18(11), e1010666. <https://doi.org/10.1371/journal.pcbi.1010666>
- McVicker, G., Praisnar, T. K., Williams, A., Wagner, N. L., Boots, M., Renshaw, S. A., & Foster, S. J. (2014). Clonal Expansion during *Staphylococcus aureus* Infection Dynamics Reveals the Effect of Antibiotic Intervention. *PLOS Pathogens*, 10(2), e1003959. <https://doi.org/10.1371/journal.ppat.1003959>
- Pappenheimer Jr., A. M. (1984). Diphtheria. In *Bacterial Vaccines* (pp. 1–36). Academic Press.
- Parveen, S., Bishai, W. R., & Murphy, J. R. (2019). *Corynebacterium diphtheriae*: Diphtheria Toxin, the *tox* Operon, and Its Regulation by Fe²⁺ Activation of apo-DtxR. *Microbiology Spectrum*, 7(4). <https://doi.org/10.1128/microbiolspec.GPP3-0063-2019>
- Pasipanodya, J. G., Mubanga, M., Ntsekhe, M., Pandie, S., Magazi, B. T., Gumede, F., Myer, L., Gumbo, T., & Mayosi, B. M. (2015). Tuberculous Pericarditis is Multibacillary and Bacterial Burden Drives High Mortality. *Ebiomedicine*, 2(11), 1634–1639. <https://doi.org/10.1016/j.ebiom.2015.09.034>
- Rello, J., Lisboa, T., Lujan, M., Gallego, M., Kee, C., Kay, I., Lopez, D., & Waterer, G. W. (2009). Severity of Pneumococcal Pneumonia

Associated With Genomic Bacterial Load. *Chest*, 136, 832–840. <https://doi.org/10.1378/chest.09-0258>

- Santos, M. I. M. A. dos, Pacheco, S. R., Stocker, A., Schinoni, M. I., Paraná, R., Reis, M. G., & Silva, L. K. (2017). Mutations associated with drug resistance and prevalence of vaccine escape mutations in patients with chronic hepatitis B infection. *Journal of Medical Virology*, 89(43), 1811–1816. <https://doi.org/10.1002/jmv.24853>
- Tiwari, T. S. P., & Wharton, M. (2012). Diphtheria Toxoid. In *Vaccines* (pp. 153–166). Elsevier.
- Wang, J., Qiu, J., Zhu, Y., Zhou, H., Yu, L., Ding, Y., Zhang, L., Guo, Z., & Dong, C. (2017). Molecular evolution of hepatitis B vaccine escape variants in China, during 2000–2016. *Vaccine*, 35(43), 5808–5813. <https://doi.org/10.1016/j.vaccine.2017.09.030>
- West, S. A., Griffin, A. S., & Gardner, A. (2007). Evolutionary Explanations for Cooperation. *Current Biology*, 17(16), R661–R672. <https://doi.org/10.1016/j.cub.2007.06.004>
- Wilson, A. D. M., Krause, J., Herbert-Read, J. E., & Ward, A. J. M. (2014). The Personality Behind Cheating: Behavioural Types and the Feeding Ecology of Cleaner Fish. *Ethology*, 120(9), 904–912. <https://doi.org/10.1111/eth12262>
- Zwart, M. P., & Elena, S. F. (2015). Matters of Size: Genetic Bottlenecks in Virus Infection and Their Potential Impact on Evolution. *Annual Review of Virology*, 2(1), 161–179. <https://doi.org/10.1146/annurev-virology-100114-055135>

Supplementary material

Stochastic model for the cooperator-cheater model

We used the model described in Equation 9 and Equation 10 to simulate the propagation of the two phenotypes, cooperator (2.1) and cheater (2.2). In these simulations, the parameters were chosen as $\alpha = 0.5$, $\eta = 0.4$, $g = 0.05$ and $\lambda = 0.2$. Three different values of $q_{2,1}$ were tested: 0.35, 0.5 and 0.75. Five initial values of $x_{2,1}$ were arbitrarily chosen and for each of these initial $x_{2,1}$ values a simulation was run with each of the three $q_{2,1}$ values. Each simulation went on for 100 time steps, one time step being equal to one generation. The population was fixed at 10,000 cells. Each time step consisted in two steps:

- Calculating the fitness value (W_i) of all of the cells using Equation 9 and Equation 10.
- Picking up the phenotype of the new 10,000 cells using a multinomial random trial where the probabilities are proportional to the values of W_i .

Then, the model continued until the final time step was reached.

Stochastic model for the adaptive dynamics model

We used the model described in Equation 1 to simulate the propagation of mutant strain(s) with different public good production phenotypes. In these simulations, the parameters were chosen as $\alpha = 0.5$, $\eta = 0.2$, $g = 0.05$ and $\lambda = 0.4$. An initial value $q = 0.75$ was used for the whole population. The simulation went on for 5,000 time steps, one time step being equal to one generation. The population was fixed at 1,000 cells. Each time step consisted in three steps:

- Establishing the list of new individuals presenting a mutation.
- Calculating the fitness value (W_i) of all of the cells using Equation 1.
- Picking up the phenotype of the new 1,000 cells using a multinomial random trial where the probabilities are proportional to the values of W_i .

Then, the model continued until the final time step was reached.

Mutations were modelled as follows: at each time step, each new cell has a certain probability of developing a mutation altering its public good production, fixed at $P_{\text{mut}} = 10^{-3}$ (so, a mutation rate $\mu = 10^{-3}$ per generation), meaning that on average one new mutation would appear per generation. For each cell presenting a mutation, its phenotype was calculated by incrementing its parent phenotype by a value picked from a uniform distribution between -0.1 and $+0.1$ (with respect to $q \in [0, 1 - g]$).

Proofs

Equation 6

We can write W_1 as a function of q_1 :

$$W_1(q_1) = (1 - q_1 - g)((1 - \eta)q_1 + g)^\alpha. \quad (22)$$

In order to find the q_1 value to maximize W_1 , we derivate W_1 , giving:

$$W_1'(q_1) = ((1 - \eta)q_1 + g)^{\alpha-1}(-(\alpha + 1)(1 - \eta)q_1 - g + \alpha(1 - \eta)(1 - g)). \quad (23)$$

In this form, the first term is positive, so the sign of W_1' is determined by the second, which is a linear function of q_1 with a slope $-(\alpha + 1)(1 - \eta) < 0$. Moreover, this term vanishes for

$$q_1^* = \frac{\alpha}{\alpha + 1} - g \frac{\alpha(1 - \eta) + 1}{(1 - \eta)(\alpha + 1)}. \quad (24)$$

Hence, the derivative is positive on $[0, q_1^*]$ and negative on $[q_1^*, 1]$. Therefore, the function W_1 reaches its maximum value on $[0, 1]$ for $q_1 = q_1^*$.

Equation 7

We know that

$$\begin{aligned} q_1^* &= \frac{\alpha}{\alpha + 1} - g \frac{\alpha(1 - \eta) + 1}{(1 - \eta)(\alpha + 1)} \\ q_1^* &= \frac{\alpha(1 - \eta) - g\alpha(1 - \eta) - g}{(1 - \eta)(\alpha + 1)} \\ q_1^* &= \frac{\alpha(g - 1)\eta + \alpha(1 - g) - g}{(1 - \eta)(\alpha + 1)}. \end{aligned} \quad (25)$$

The denominator is always positive because $0 \leq \eta \leq 1$ and $\alpha > 0$, so q_1^* has the same sign as its numerator. The numerator is a linear function of η with the slope $\alpha(g - 1) \leq 0$ (because $g \leq 1$) and vanishes for

$$\eta'_1 = 1 - \frac{g}{\alpha(1 - g)}. \quad (26)$$

Therefore, q_1^* is positive when $\eta \leq \eta'_1$ and negative when $\eta \geq \eta'_1$.

Equation 16

We search the value $x_{2.1}$ for which $W_{2.1} = W_{2.2}$. We posit $C_{2.1} = 1 - q_{2.1} - g$ and $C_{2.2} = 1 - g$ and we have

$$\begin{aligned} W_{2.1} &= W_{2.2} \\ \Leftrightarrow C_{2.1}((1 - \lambda)(1 - \eta)q_{2.1} + g + \lambda(1 - \eta)x_{2.1}q_{2.1})^\alpha &= C_{2.2}(g + \lambda(1 - \eta)x_{2.1}q_{2.1})^\alpha \\ \Leftrightarrow C_{2.1}^{\frac{1}{\alpha}}((1 - \lambda)(1 - \eta)q_{2.1} + g + \lambda(1 - \eta)x_{2.1}q_{2.1}) &= C_{2.2}^{\frac{1}{\alpha}}(g + \lambda(1 - \eta)x_{2.1}q_{2.1}) \\ \Leftrightarrow C_{2.1}^{\frac{1}{\alpha}}((1 - \lambda)(1 - \eta)q_{2.1} + g) + C_{2.1}^{\frac{1}{\alpha}}\lambda(1 - \eta)x_{2.1}q_{2.1} &= C_{2.2}^{\frac{1}{\alpha}}g + C_{2.2}^{\frac{1}{\alpha}}\lambda(1 - \eta)x_{2.1}q_{2.1} \\ \Leftrightarrow C_{2.1}^{\frac{1}{\alpha}}\lambda(1 - \eta)x_{2.1}q_{2.1} - C_{2.2}^{\frac{1}{\alpha}}\lambda(1 - \eta)x_{2.1}q_{2.1} &= C_{2.2}^{\frac{1}{\alpha}}g - C_{2.1}^{\frac{1}{\alpha}}((1 - \lambda)(1 - \eta)q_{2.1} + g) \\ \Leftrightarrow x_{2.1} \left(C_{2.1}^{\frac{1}{\alpha}}\lambda(1 - \eta)q_{2.1} - C_{2.2}^{\frac{1}{\alpha}}\lambda(1 - \eta)q_{2.1} \right) &= C_{2.2}^{\frac{1}{\alpha}}g - C_{2.1}^{\frac{1}{\alpha}}((1 - \lambda)(1 - \eta)q_{2.1} + g) \\ \Leftrightarrow x_{2.1} &= \frac{C_{2.2}^{\frac{1}{\alpha}}g - C_{2.1}^{\frac{1}{\alpha}}((1 - \lambda)(1 - \eta)q_{2.1} + g)}{C_{2.1}^{\frac{1}{\alpha}}\lambda(1 - \eta)q_{2.1} - C_{2.2}^{\frac{1}{\alpha}}\lambda(1 - \eta)q_{2.1}}. \end{aligned} \quad (27)$$

Reorganizing the last line of Equation 27 and recalling that $C_{2.1} = 1 - q_{2.1} - g$ and $C_{2.2} = 1 - g$, we eventually obtain the value of $x_{2.1}^*$ as

$$x_{2.1}^* = \frac{(1 - q_{2.1} - g)^{\frac{1}{\alpha}}((1 - \lambda)(1 - \eta)q_{2.1} + g) - (1 - g)^{\frac{1}{\alpha}}g}{\lambda(1 - \eta) \left((1 - g)^{\frac{1}{\alpha}} - (1 - q_{2.1} - g)^{\frac{1}{\alpha}} \right) q_{2.1}}. \quad (28)$$

Equation 19

We can interpret the function $\omega_{3.2}$ as a function of two variables,

$$\begin{aligned} F(q_{3.1}, q_{3.2}) &:= (1 - q_{3.2} - g)((1 - \lambda)(1 - \eta)q_{3.2} + g + \lambda(1 - \eta)q_{3.1})^\alpha \\ &\quad - (1 - q_{3.1} - g)((1 - \eta)q_{3.1} + g)^\alpha \end{aligned} \quad (29)$$

where $q_{3,1}$ represents the public good production of the resident cell and $q_{3,2}$ the public good production of a mutant cell. We can easily verify for all $q_{3,1} \in [0, 1]$, $F(q_{3,1}, q_{3,1}) = 0$ which is consistent with the biological meaning of F . We call $f_{q_{3,1}} : q_{3,2} \mapsto F(q_{3,1}, q_{3,2})$ the function that gives the invasion fitness as a function of the mutant cell's public good production $q_{3,2}$, for a fixed resident cell public good production $q_{3,1}$. The singular value we seek corresponds to a resident public good production that cannot be invaded by any mutant. Mathematically, this amounts to finding a value $q_{3,1}^*$ such that $f_{q_{3,1}}^*(q_{3,2}) \leq 0, \forall q_{3,2} \in [0, 1]$.

Let us show, using a Analysis-Synthesis reasoning, that there exists a unique $q_{3,1}^*$ value in $]0, 1[$, the boundary cases being trivial.

Analysis: Assume that there exists a value $q_{3,1}^* \in]0, 1[$ such that $f_{q_{3,1}^*}(q_{3,2}) \leq 0, \forall q_{3,2} \in [0, 1]$. Since $f_{q_{3,1}^*}(q_{3,1}^*) = F(q_{3,1}^*, q_{3,1}^*) = 0$, it implies that $q_{3,1}^*$ is a minimum of the function on the open interval $]0, 1[$. Therefore, its derivative vanishes at this point $f'_{q_{3,1}^*}(q_{3,1}^*) = 0$ and

$$f_{q_{3,1}^*}(q_{3,2}) = (1 - q_{3,2} - g)((1 - \lambda)(1 - \eta)q_{3,2} + \lambda(1 - \eta)q_{3,1}^* + g)^\alpha - (1 - q_{3,1}^* - g)((1 - \eta)q_{3,1}^* - g)^\alpha. \quad (30)$$

So we compute the derivative

$$f'_{q_{3,1}^*}(q_{3,2}) = -((1 - \lambda)(1 - \eta)q_{3,2} + \lambda(1 - \eta)q_{3,1}^* + g)^\alpha + (1 - q_{3,2} - g)\alpha(1 - \lambda)(1 - \eta)((1 - \lambda)(1 - \eta)q_{3,2} + \lambda(1 - \eta)q_{3,1}^* + g)^{\alpha-1}, \quad (31)$$

and then apply to $q_{3,2} = q_{3,1}^*$:

$$\begin{aligned} f'_{q_{3,1}^*}(q_{3,1}^*) &= -((1 - \eta)q_{3,1}^* + g)^\alpha + (1 - q_{3,1}^* - g)\alpha(1 - \lambda)(1 - \eta)((1 - \eta)q_{3,1}^* + g)^{\alpha-1} \\ &= ((1 - \eta)q_{3,1}^* + g)^{\alpha-1}(- (1 - \eta)q_{3,1}^* - g + (1 - g)\alpha(1 - \lambda)(1 - \eta) \\ &\quad - q_{3,1}^*\alpha(1 - \lambda)(1 - \eta)). \end{aligned} \quad (32)$$

We know $f'_{q_{3,1}^*}(q_{3,1}^*) = 0$, however, $(1 - \eta)q_{3,1}^* + g > 0$ and $\lambda \neq 1$ so

$$\begin{aligned} &-\frac{(1 - \eta)q_{3,1}^*}{1 - \lambda} - \frac{g}{1 - \lambda} + (1 - g)\alpha(1 - \eta) - q_{3,1}^*\alpha(1 - \lambda)(1 - \eta) = 0 \\ \Leftrightarrow q_{3,1}^* \left(\frac{(1 - \eta)}{1 - \lambda} + \alpha(1 - \eta) \right) &= (1 - g)\alpha(1 - \eta) - \frac{g}{1 - \lambda} \\ \Leftrightarrow q_{3,1}^* &= \frac{(1 - g)\alpha(1 - \eta)}{\alpha(1 - \eta) + \frac{1 - \eta}{1 - \lambda}} - g \frac{1}{(1 - \eta) + \alpha(1 - \eta)(1 - \lambda)} \\ \Leftrightarrow q_{3,1}^* &= \frac{\alpha}{\alpha + \frac{1}{1 - \lambda}} - g \frac{\alpha(1 - \eta) + (1, 1 - \lambda)}{(1 - \eta)(\alpha + \frac{1}{1 - \lambda})}. \end{aligned} \quad (33)$$

If $q_{3,1}^*$ exists, it must have this form and therefore is unique.

Synthesis: Let $q_{3,1}^*$ as in the last line of Equation 33, let us verify $f_{q_{3,1}^*}(q_{3,2}) \leq 0, \forall q_{3,2} \in [0, 1]$. From Equation 33 we can write the derivative of f in the form

$$f'_{q_{3,1}^*}(q_{3,2}) = ((1 - \lambda)(1 - \eta)q_{3,2} + \lambda(1 - \eta)q_{3,1}^* + g)^{\alpha-1} \times [-(1 - \lambda)(1 - \eta)(\alpha + 1)q - (1 - \eta)(\lambda q_{3,1}^* - (1 - g)(1 - \lambda)\alpha) - g]. \quad (34)$$

The first term is always positive, as it is a sum of positive terms; therefore, the derivative has the same sign as the second term. The second term is linear in $q_{3,2}$ with a slope $-(1 - \lambda)(1 - \eta)(\alpha + 1) < 0$ and vanishes at $q_{3,1}^*$ (which is easily verified). Hence, the derivative is positive on $[0, q_{3,1}^*]$ and

negative on $[q_{3.1}^*, 1]$. Therefore, the function is increasing on $[0, q_{3.1}^*]$ and decreasing on $[q_{3.1}^*, 1]$. Since $f_{q_{3.1}^*}(q_{3.1}^*) = 0$, the function is always negative on $[0, 1]$. Thus, the expression of $q_{3.1}^*$ in the last line of Equation 33 satisfies $f_{q_{3.1}^*}(q_{3.2}) \leq 0, \forall q \in [0, 1]$.

Conclusion: There exists one and only one value of production of public good $q_{3.1}^*$ for which the phenotype cannot be invaded, the form of $q_{3.1}^*$ is

$$q_{3.1}^* = \frac{\alpha}{\alpha + \frac{1}{1-\lambda}} - g \frac{\alpha(1-\eta) + \frac{1}{1-\lambda}}{(1-\eta)(\alpha + \frac{1}{1-\lambda})}. \quad (35)$$

Equation 20

Similarly to the previous case (see proof of Equation 7), $q_{3.1}^*$ can be expressed as a function of η as

$$q_{3.1}^* = \frac{\eta\alpha(g-1) + \alpha - g\alpha - \frac{g}{1-\lambda}}{(1-\eta)(\alpha + \frac{1}{1-\lambda})}. \quad (36)$$

In this form, the denominator is positive, so the sign of $q_{3.1}^*$ is determined by the numerator, which is a linear function of η with a slope $\alpha(g-1) < 0$. Moreover, the numerator vanishes for

$$\eta'_{3.1} = 1 - \frac{g}{\alpha(1-\lambda)(1-g)}. \quad (37)$$

Therefore, $q_{3.1}^*$ is positive when $\eta \leq \eta'_{3.1}$ and negative when $\eta \geq \eta'_{3.1}$.